Dispersion irrelevant wideband asymmetric transmission in dielectric photonic crystal gratings

Andriy E. Serebryannikov,[1,*] Evrim Colak,[2] A. Ozgur Cakmak,[2] and Ekmel Ozbay[2]

[1]*Department of Electrical Engineering, Hamburg University of Technology, Denickestrasse 22, Hamburg D-21073, Germany*

[2]*Nanotechnology Research Center, Bilkent University, Ankara 06800, Turkey*

**Corresponding author: serebryannikov@tu-harburg.de*

Received July 25, 2012; accepted October 2, 2012;
posted October 23, 2012 (Doc. ID 173185); published November 22, 2012

Wideband suppression of zero order and relevant strongly asymmetric transmission can be obtained in photonic crystal gratings that are made of linear isotropic materials and show the broken structural (axial) symmetry, even if zero diffraction order may be coupled to a Floquet–Bloch (FB) wave at the incidence and exit interfaces. The studied mechanism requires that the peculiar diffractions at the corrugated exit interface inspire strong energy transfer to higher orders, including those not coupled to an FB wave. At the opposite direction of incidence, transmission due to zero and some higher orders that may be coupled at the corrugated input interface can vanish. This leads to the alternative scenario of wideband unidirectional transmission, which itself does not need but can coexist with the other scenario based on the merging of asymmetric diffraction and dispersion of the FB mode.

OCIS codes: 050.1950, 050.1960, 050.5298, 120.7000.

Among the mechanisms enabling partial analogs of diodelike transmission, which is usually associated with the use of anisotropic [1,2] and/or nonlinear [3,4] materials, the diffraction [5–7] and polarization conversion [8] relevant mechanisms of asymmetric transmission should be mentioned. These mechanisms need the structures with the broken symmetry, which are made of linear isotropic materials and, thus, show the Lorentz reciprocity. They could be considered as nonreciprocal in a wider sense, since forward and backward transmissions are strongly distinguished [6,9]. In particular, the diffraction relevant asymmetry in transmission originates from asymmetry in the coupling conditions at the incidence and the exit interfaces, leading to different contributions of the same higher diffraction orders at the two opposite directions of incidence.

Metallic gratings [5] and especially photonic crystal (PhC) gratings [6,10] with different periods of input and exit interfaces are the perfect candidates for obtaining the asymmetric transmission. For the latter, the merging effects of the dispersion of Floquet–Bloch (FB) modes of the PhC and diffractions can result in wideband suppression of the unwanted diffraction orders that may propagate in the incidence half-space but originally are not coupled to FB waves. Thus, they do not appear in transmission, provided that the properly designed exit interface itself results in fewer orders that may propagate in the exit half-space than in the input one. Nonsymmetric PhC gratings (see Fig. 1) were suggested for transmission less than a decade ago [11] and then studied with the emphasis put on asymmetric transmission at zero and nonzero angles of incidence [6]. The advanced performances were later studied in various frequency ranges from acoustic to optical ones [7,9,10,12].

In the direct regime [10], the wideband unidirectionality with high forward-case transmittance (corrugated-side illumination), $T^{\rightarrow} \neq 0$, and vanishing backward-case transmittance (noncorrugated-side illumination), $T^{\leftarrow} = 0$, occurs while zero order (symmetric) transmission is suppressed, $t_0^{\rightarrow} = t_0^{\leftarrow} = 0$. This regime is realizable in the nonsymmetric PhC gratings due to the common effect of diffraction and dispersion of FB modes.

Recently it has been shown that the inverse regime of unidirectional transmission, i.e., that with $T^{\leftarrow} \neq 0$ and $T^{\rightarrow} \approx 0$, can appear—in line with the Lorentz reciprocity—in the same structures as the direct one but at a fixed frequency [10]. In this scenario, zero order is coupled to an FB wave for both of the (opposite) illumination directions, but extreme conversion into higher-order transmitted beams occurs at the corrugated exit interface. The question remains open whether suppression of zero order and the associated symmetric transmission component can be wideband regarding frequency and angle of incidence θ. An attempt to obtain the reversible unidirectional transmission, i.e., that with $T^{\leftarrow} = 0$ and $T^{\rightarrow} \neq 0$ in one, and that with $T^{\rightarrow} = 0$ and $T^{\leftarrow} \neq 0$ in the other among the two adjacent frequency or/and angle ranges, is the next step toward new functionalities. Since wideband suppression of t_0 cannot be obtained due to the above-mentioned merging in both of the cases simultaneously, suppression of t_0 should be realized in one of these ranges solely due to the diffractions (i.e., not due to dispersion of FB modes). Such a wideband regime has not yet been found.

In this Letter, we demonstrate that the strongly pronounced, wideband asymmetric transmission can be obtained in the inverse regime, including the diodelike case when the transmission is vanishing in one of the two

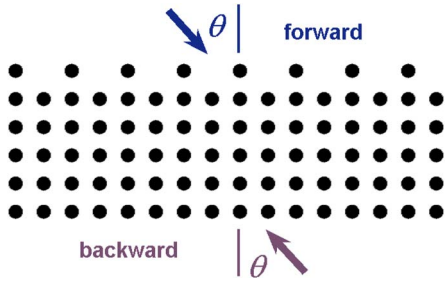

Fig. 1. (Color online) Geometry of PhC grating with one-side corrugations.

opposite directions of incidence. It is connected with the peculiar diffractions obtainable at a proper adjustment of the PhC lattice and corrugation parameters. In contrast to the direct regime, which is usually studied for the PhC gratings, the suppression of certain diffraction orders is not connected with the restrictions dictated by the dispersion of FB modes and wave vector diagrams. We focus on the cases when not only zero order (symmetric transmission component) but also some of the higher orders contributing to the asymmetric component can be suppressed in the forward transmission, even if the wave vector diagram allows them to couple to an FB wave at the input and the exit interface. We consider diffraction on PhC gratings based on the square-lattice PhCs that consist of the dielectric rods of diameter d and permittivity ε_r. There are P layers of the rods. Since one of the interface layers has a larger lateral period ($L = 2a$) than all the other layers whose periods are equal to lattice constant a, as in Fig. 1, the grating is axially nonsymmetric. Plane wave illumination with the electric field vector along the rods is considered. Simulations are performed by using an integral equation technique [13].

Figure 2 presents n-order forward ($t_n^{\rightarrow}$) and backward ($t_n^{\leftarrow}$) transmittances versus kL (k stands for the free-space wave number) for the PhC grating that has similar parameters as one of those in [7,10]. In the general case, the exit interface with a larger period than the input one can provide the contribution of such diffraction orders to the transmissions that have been either evanescent or propagating but uncoupled at the input interface. In turn, a smaller exit period than the input one cannot close the transmission channels that are open due to the input interface. In case of the backward transmission in Fig. 2(a), the wave vector diagram (not shown) allows the orders with $n = 0$ and $n = -2$ to be coupled to one of the FB waves at the input (noncorrugated) interface, nearly at $7.8 < kL < 8.4$. In turn, $t_{-1}^{\leftarrow}$ can contribute to $T^{\leftarrow}$ only due to the effect of the exit (corrugated) interface. Variation in d/a allows one to control the strength of the conversing effect of the exit interface. One can see that $t_{-1}^{\leftarrow}$ can dominate in $T^{\leftarrow}$. In case of the forward transmission in Fig. 2(b), the orders with $n = 0$, -1, and -2 may be coupled to the same FB wave in this kL range at the input (corrugated) interface. However, only one of the associated three opened transmission channels actually contributes to $T^{\rightarrow}$. Thus, we obtain a wide kL range, in which $T^{\rightarrow} \approx t_{-1}^{\rightarrow}$ and $T^{\leftarrow} \approx t_{-1}^{\leftarrow} + t_{-2}^{\leftarrow}$, i.e., zero order is suppressed.

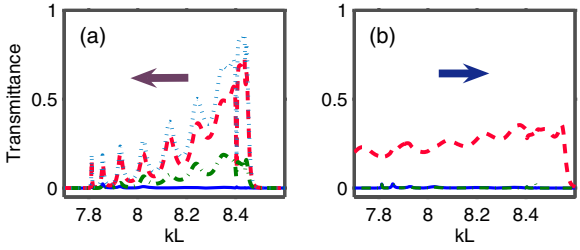

Fig. 2. (Color online) (a) Backward and (b) forward transmittance at $d/a = 0.53$, $\varepsilon_r = 9.61$, $P = 12$, and $\theta = 60°$. Blue solid curve, $t_0 = t_0^{\leftarrow} = t_0^{\rightarrow} \approx 0$; red dashed curve, (a) $t_{-1}^{\leftarrow}$ and (b) $t_{-1}^{\rightarrow}$; green dash-dotted curve, (a) $t_{-2}^{\leftarrow}$ and (b) $t_{-2}^{\rightarrow} \approx 0$; cyan dotted curve, (a) $T^{\leftarrow}$.

The observed asymmetric transmission range can be thought of as a partial analog of the known one-way bands with $T^{\rightarrow} \approx t_0$ and $T^{\leftarrow} \approx t_0 + t_{-1}^{\leftarrow} + t_{+1}^{\leftarrow}$ at $\theta = 0°$ [5,6]. The first negative order in Fig. 2 plays the role similar to that of zero order in [5,6], i.e., it contributes to both $T^{\rightarrow}$ and $T^{\leftarrow}$. However, in our case, the two-way transmission component is asymmetric, i.e., $t_{-1}^{\rightarrow} \neq t_{-1}^{\leftarrow}$. In Fig. 2(b) the three ranges of $T^{\rightarrow} \approx t_{-1}^{\rightarrow}$ merge. These ranges are associated with the diffraction relevant suppression of zero order at (i) $7.8 < kL < 8.4$, and the uncoupling of zero order to an FB wave at the input interface at (ii) $kL < 7.8$ and (iii) $kL > 8.4$. Such a merging can be observed in a wide range of parameter variations. Roughly, these three regimes correspond—within transition ranges—to the (not shown) isofrequency contours (IFCs) located around (i) Γ point (being narrower than in air), (ii) Γ and M points, and (iii) X point, i.e., similarly to Figs. 1(a), 1(d), and 1(b) in [10], respectively.

The above-presented results show that the wideband suppression of zero order and the relevant asymmetric transmission can be obtained without the blocking effect connected with the specific dispersion of the FB mode, as in [6,10]. However, this does not guarantee that $T^{\rightarrow} \approx 0$ and $T^{\leftarrow} \neq 0$, as required for obtaining a diodelike operation regime in a wide kL range. Thus, a further adjustment is needed. Two examples are presented in Fig. 3. Here, the lattice parameters are either the same as or close to those in [7]. One can see the range of unidirectional transmission with $T^{\rightarrow} \approx 0$ and $T^{\leftarrow} \approx t_{-1}^{\leftarrow} + t_{-2}^{\leftarrow}$ in the vicinity of $kL = 8.5$. In both of the forward and backward cases, the orders with $n = 0$ and $n = -2$ may be coupled to the FB wave at the input interface. The IFCs (not shown) are located around the M point and have a nearly square shape, as those used earlier in bandpass spatial filtering [14] and direct regime of unidirectional transmission [6]. In turn, the order with $n = -1$ contributes to $T^{\leftarrow}$ due to the coupling at the exit (corrugated) interface. Furthermore, although the order with $n = -2$ is itself coupled to the FB wave in a two-way manner, we obtain $t_{-2}^{\leftarrow} \gg t_{-2}^{\rightarrow}$. Hence, the effect of the corrugated interface

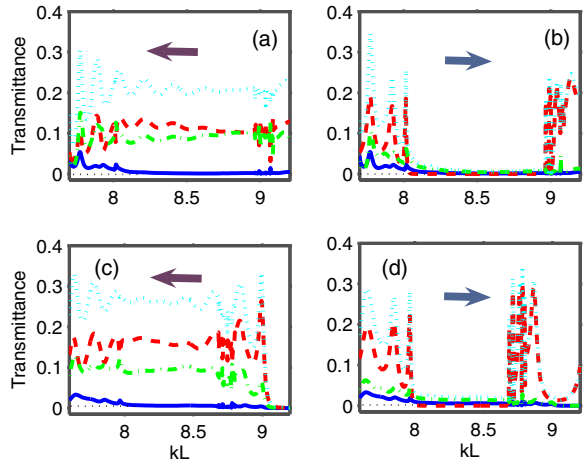

Fig. 3. (Color online) (a), (c) Backward and (b), (d) forward transmittance at (a), (b) $d/a = 0.4$ and (c), (d) $d/a = 0.43$, $\varepsilon_r = 5.8$, $P = 12$, and $\theta = 60°$. Blue solid curve, $t_0 = t_0^{\leftarrow} = t_0^{\rightarrow}$; red dashed curve, (a), (c) $t_{-1}^{\leftarrow}$ and (b), (d) $t_{-1}^{\rightarrow}$; green dash-dotted curve, (a), (c) $t_{-2}^{\leftarrow}$ and (b), (d) $t_{-2}^{\rightarrow}$; cyan dotted curve, (a), (c) $T^{\leftarrow}$ and (b), (d) $T^{\rightarrow}$.

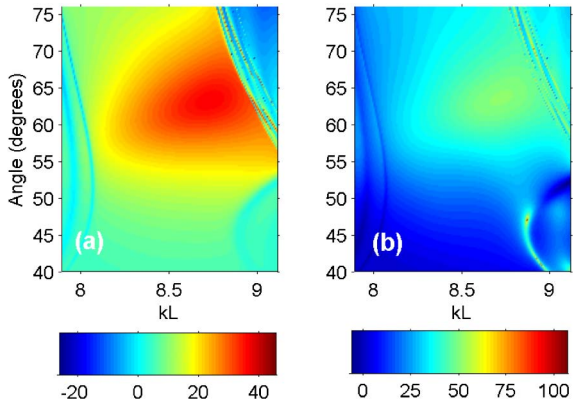

Fig. 4. (Color online) Maps of (a) backward-to-forward transmittance contrast, $C_1 = T^{\leftarrow}/T^{\rightarrow}$, and (b) higher to zero order transmittance contrast in the backward case, $C_2 = (t_{-1}^{\leftarrow} + t_{-2}^{\leftarrow})/t_0$, in dB, for the same PhC grating as in Figs. 3(a) and 3(b).

manifests itself also in the coupling strength. Another adjustment is required for increasing $T^{\leftarrow}$ when $T^{\rightarrow} \approx 0$ and obtaining the switching between the wideband regimes with $T^{\leftarrow} \neq 0$ and $T^{\rightarrow} \approx 0$, and $T^{\leftarrow} = 0$ and $T^{\rightarrow} \neq 0$.

For practical applications, it is important to estimate the extent to which the studied asymmetric transmission regime is sensitive to variations in d/a and θ. As follows from the obtained results, the inverse unidirectional regime exists at least if d/a is varied from 0.27 to 0.43. In order to demonstrate the bandwidth and effect of θ, Fig. 4 presents the two contrasts, C_1 and C_2, that characterize the asymmetry in transmission at the simultaneous variation of kL and θ. Both of the contrasts are quite high in the considered ranges of kL and θ variation. Furthermore, there is strong correlation between C_1 and C_2. C_1 is the highest in the vicinity of $\theta = 63°$. Here, the bandwidth is about 11%. The results obtained for the inverse regime show that unidirectionality can appear in a wide range of parameter variations. This gives one significant freedom in choice of the parameters of PhC and illumination. Thus, the inverse regime might be even more preferable than the direct regime, although higher efficiency can be obtained for the latter.

To summarize, we demonstrated that the wideband asymmetric transmission can appear in a nonsymmetric PhC grating in the inverse regime as a purely diffraction effect. The obtained results include the case of unidirectional transmission, in which the transmission vanishes for one of the two opposite incidence directions. This is distinguished from the direct regime, which occurs due to the merging of the diffraction and dispersion effects. It is shown that zero order being responsible for the symmetric transmission may be coupled to an FB wave at the incidence interface in both of the forward and backward cases, but its contribution to the transmission is negligible. In turn, the contributions of the higher orders, which are asymmetric due to the structural (axial) asymmetry, can be significant and strongly dependent on the choice of the incidence direction. The studied mechanism is quite tolerant with respect to the variations in the angle of incidence and rod-diameter-to-lattice-constant ratio. The obtained results confirm the principal possibility of designing switchable diodelike devices in which the directions of the nonvanishing transmission are opposite for the two neighboring wide frequency ranges.

References

1. Z. Wang, J. D. Chong, J. D. Joannopoulos, and M. Soljacic, Phys. Rev. Lett. **100**, 013905 (2008).
2. A. Figotin and I. Vitebskiy, Phys. Rev. B **67**, 165210 (2003).
3. M. Scalora, J. P. Dowling, C. M. Bowden, and M. J. Bloemer, J. Appl. Phys. **76**, 2023 (1994).
4. M. Soljacic, C. Luo, J. D. Joannopoulos, and S. Fan, Opt. Lett. **28**, 637 (2003).
5. M. J. Lockyear, A. P. Hibbins, K. R. White, and J. R. Sambles, Phys. Rev. E **74**, 056611 (2006).
6. A. E. Serebryannikov, Phys. Rev. B **80**, 155117 (2009).
7. A. O. Cakmak, E. Colak, A. E. Serebryannikov, and E. Ozbay, Opt. Express **18**, 22283 (2010).
8. M. Mutlu, A. E. Akosman, A. E. Serebryannikov, and E. Ozbay, Phys. Rev. Lett. **108**, 213905 (2012).
9. C. Lu, X. Hu, and Q. Gong, Opt. Lett. **36**, 4668 (2011).
10. A. E. Serebryannikov, A. O. Cakmak, and E. Ozbay, Opt. Express **20**, 14980 (2012).
11. A. E. Serebryannikov, T. Magath, and K. Schuenemann, Phys. Rev. E **74**, 066607 (2006).
12. X. F. Li, X. Ni, L. Feng, M. H. Lu, C. He, and Y. F. Chen, Phys. Rev. Lett. **106**, 084301 (2011).
13. T. Magath and A. E. Serebryannikov, J. Opt. Soc. Am. A **22**, 2405 (2005).
14. A. E. Serebryannikov, A. Y. Petrov, and E. Ozbay, Appl. Phys. Lett. **94**, 181101 (2009).